2012

A Simulation Model for the Application of Nanofluids as Condenser Coolants in Vapor Compression Heat Pumps

José Alberto Reis Parise
parise@puc-rio.br

A Simulation Model for the Application of Nanofluids as Condenser Coolants in Vapor Compression Heat Pumps

José Alberto Reis PARISE[1]*, Ricardo Fernando Paes TIECHER[2]

[1]Pontifícia Universidade Católica do Rio de Janeiro, Department of Mechanical Engineering,
22453-900, Rio de Janeiro, RJ, Brazil
Phone: +5521-35271380, Fax: +5521-35271165, E-mail: parise@puc-rio.br

[2]Pontifícia Universidade Católica do Rio de Janeiro, Department of Mechanical Engineering,
22453-900, Rio de Janeiro, RJ, Brazil
Phone: +5521-35271162, Fax: +5521-35271165, E-mail: ricardo.tiecher@aluno.puc-rio.br

ABSTRACT

A simulation model was developed for the performance prediction of a vapor compression heat pump using nanoscale colloidal solutions (nanofluids) as condenser coolants. The model was intended for a liquid-to-liquid heat pump, with reciprocating compressor, thermostatic expansion valve and counter-flow double-tube condenser and evaporator. The compressor is characterized (input data) by its swept volume, shaft speed and isentropic and volumetric efficiencies curves, and the expansion device, by the evaporator superheat. The condenser is divided into three zones, desuperheating, condensing and subcooling. Likewise, the evaporator is divided into the boiling and superheating zones. The heat exchangers are characterized (input data) by their geometry (inner and outer tube diameters and length). Operational input data also include condenser subcooling and heat transfer fluids (condenser and evaporator) mass flow rates and inlet thermodynamic states. A computational program was developed to solve the resulting non-linear system of algebraic equations. Solution of the system provides the cycle overall thermal performance, as well as condensing and evaporating pressures and the thermodynamic states of refrigerant and heat transfer fluids at all points of the cycle. Preliminary results were obtained for the simulation of a 19 kW nominal capacity water-to-water/(H_2O-Cu nanofluid) heat pump. A 5.4% increase in the heating coefficient of performance, for a typical operating condition, was predicted for a nanoparticle volume fraction of 2%.

1. INTRODUCTION

This paper studies the application of nanofluids as condenser coolants of vapor compression heat pumps. Nanofluids are nanoscale colloidal solutions, consisting of nanoparticles (with sizes of the order of 1 to 100 nm) dispersed in a base fluid (Choi, 1995; Cheng et al, 2008). If compared to their corresponding base-fluid, nanofluids present an uncontested enhancement in thermal conductivity, viscosity and density, as now reported in a number of research papers and reviews (e.g., Khanafer and Vafai, 2011). Heat transfer in nanofluids (laminar or turbulent flow; natural or forced convection; single phase, pool boiling, nucleate boiling or critical heat flux) has also been investigated worldwide. For the purpose of the present simulation, i.e., single-phase forced convective flow, literature results conclude that, in general, conventional pressure drop correlations still apply to nanofluids, whereas new correlations for the Nusselt number, or even new heat transfer mechanisms (such as from Buongiorno, 2006), must be sought (see, for example, Sarkar, 2011). Papers on applications of nanofluids are found in smaller numbers and, more specifically, the study on their use as heat transfer fluids in vapour compression cycles is still incipient. An exploratory simulation was carried out by Loaiza et al (2010), who numerically studied the use of nanofluids as secondary fluids (i.e., heat transfer fluids exchanging heat with the refrigerant in the evaporator) in vapour compression refrigeration systems. The present paper improves the model from Loaiza et al. (2010) by allowing more realistic situations to be predicted (for example, variable condensing and evaporating pressures, to be determined as a result of operational and fluid conditions, including nanofluid characteristics).

2. MATHEMATICAL MODEL

The mathematical model here employed has already been outlined in Parise (2010) and Loaiza et al (2010). It was updated to meet the specific objectives of the present study.

2.1 Control Volumes

Figure 1a depicts a typical vapor compression heat pump cycle operating with liquid circuits at both the evaporator (secondary fluid) and condenser (coolant). Seven control volumes comprise the system, namely: compressor (cp), condenser´s desuperheating (ds), condensing (cs) and subcooling (sc) zones, expansion device (xd) and evaporator´s zones, boiling (bo) and superheating (sh). The P-h diagram of the cycle, with corresponding control volumes and refrigerant thermodynamic states, is presented in Figure 1b.

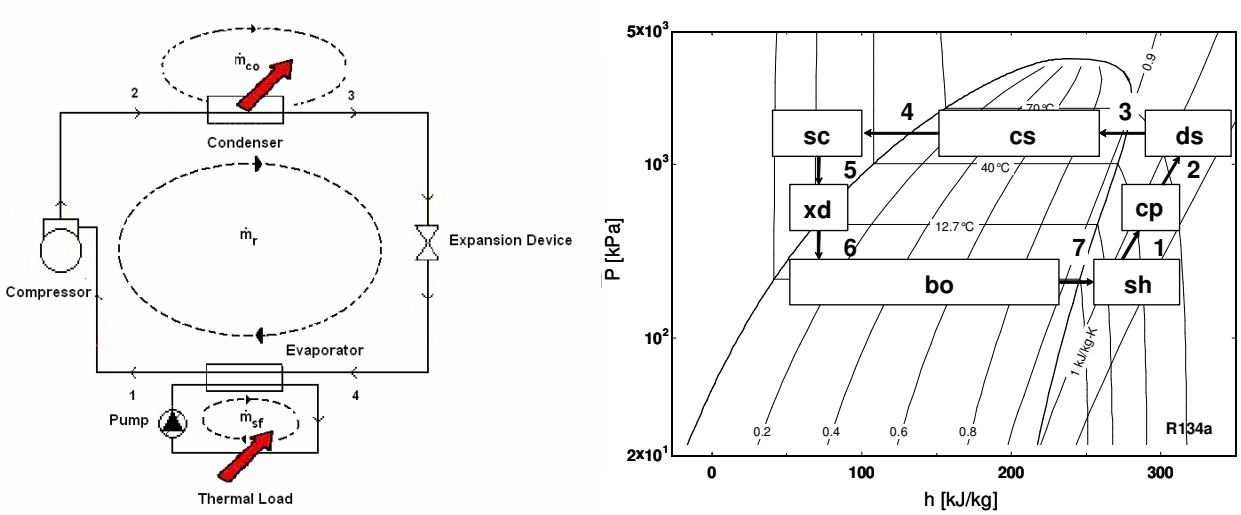

Figure 1: a) Vapor compression heat pump system with secondary fluid and condenser coolant; b) Control volumes and refrigerant states depicted in the P-h diagram. Refrigerant states: 1 – compressor suction; 2 – compressor discharge; 3 – start of condensation (or dew point, for mixtures); 4 – condenser saturated liquid or, for mixtures, bubble point; 5 – condenser outlet; 6 – evaporator inlet; 7 – evaporator dry-out point.

2.2 Compressor

A simple efficiency-based model is employed for the compressor. In order to determine the refrigerant state at compressor discharge, an empirical curve (e.g., Brown et al., 2002) is provided for the isentropic efficiency, which is related to compressor suction and discharge thermodynamic states as follows:

$$\eta_{s,cp} = \frac{(h_{2s} - h_1)}{(h_2 - h_1)};\ s_{2s} = s_1;\ \eta_{s,cp} = b_1 + b_2\,\theta_{cp};\ \theta_{cp} = \frac{P_2}{P_1} \tag{1}$$

With an empirical equation for the volumetric efficiency (Brown et al., 2002), written in terms of the pressure ratio and specific heat ratio, the refrigerant mass flow rate is determined by:

$$\dot{m}_{rf} = \eta_v v_1 \dot{V}_{cp} = \eta_v\, v_1\, n_p \left(\frac{\pi D_p^2}{4} s_p\right)\frac{N}{60};\ \eta_{v,cp} = a_1\left[1 - a_2\left(\theta_{cp}^{1/\gamma} - 1\right)\right];\ \gamma = \frac{c_p}{c_v} \tag{2}$$

Finally, compressor adiabatic work and power consumption are determined from:

$$\dot{W}_{cp} = \dot{m}_{rf}\, w_{cp}\, \eta_{em};\ w_{cp} = h_2 - h_1 \tag{3}$$

2.3 Condenser

2.3.1 Heat transfer: Each zone of the condenser, Figure 2, is treated as an independent heat exchanger, with its own refrigerant and cooling fluid energy balance equations, as well as the heat transfer rate and effectiveness equation (e.g., Martins Costa and Parise, 1993). Overall counter-flow is assumed.

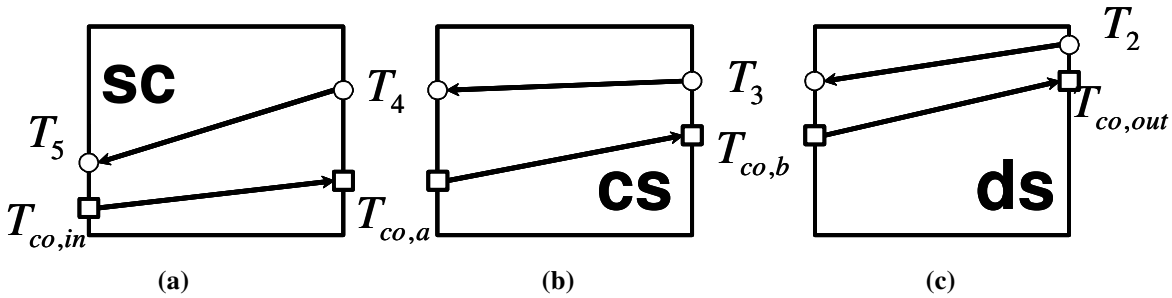

Figure 2: Control volumes for the condenser (desuperheater, ds, condensing zone, cs, and subcooler, sc).

Equations (4) and (5) describe the gas-to-gas and liquid-to-gas single-phase heat exchange in the desuperheating and subcooling zones, respectively. Equations (6) and (7) provide the zones effectiveness (counter-flow single-phase heat transfer) equations.

$$\dot{Q}_{ds} = \dot{m}_{co}\, c_{p,co}\left(T_{co,out} - T_{co,b}\right);\ \dot{Q}_{ds} = \dot{m}_{rf}\left(h_2 - h_3\right);\ \dot{Q}_{ds} = C_{\min,ds}\,\varepsilon_{ds}\left(T_2 - T_{co,b}\right) \tag{4}$$

$$\dot{Q}_{sc} = \dot{m}_{rf}\left(h_4 - h_5\right);\ \dot{Q}_{sc} = \dot{m}_{co}\, c_{p,co}\left(T_{co,a} - T_{co,in}\right);\ \dot{Q}_{sc} = C_{\min,sc}\,\varepsilon_{sc}\left(T_4 - T_{co,in}\right) \tag{5}$$

$$\varepsilon = \frac{1-\exp\left[-NTU\left(1-C^*\right)\right]}{1-C^*\left[-NTU\left(1-C^*\right)\right]}\ or\ \varepsilon = \frac{NTU}{NTU+1},\ \text{if } C^* = 1 \tag{6}$$

$$C_{\min,ds} = \min\left(\dot{m}_{co}c_{p,co};\dot{m}_{rf}c_{p,v,ds}\right);\ C_{\min,sc} = \min\left(\dot{m}_{co}c_{p,co};m_{rf}c_{p,l,sc}\right);\ C^* = \frac{C_{\min}}{C_{\max}};\ NTU = \frac{U\,A}{C_{\min}} \tag{7}$$

The condensing control volume (cs), given the variation of the refrigerant-side heat transfer coefficient with the local vapor quality, was further divided into a number of small control volumes of equal specific enthalpy increment, Figure 3, for which the following equations apply:

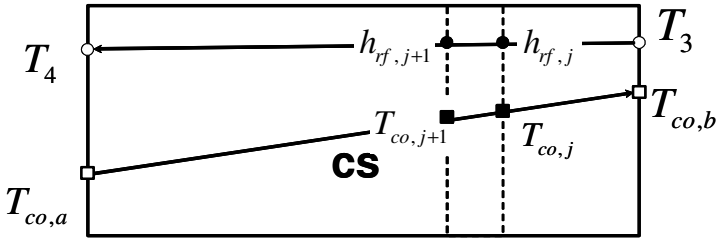

Figure 3: Heat transfer element in the condenser two-phase zone (*cs*).

$$\dot{Q}_{cs,j} = \dot{m}_{rf}\left(h_{rf,j} - h_{rf,j+1}\right);\ \dot{Q}_{cs,j} = \dot{m}_{co}\, c_{p,co}\left(T_{co,j} - T_{co,j+1}\right);\ \dot{Q}_{cs,j} = \dot{m}_{co}\, c_{p,co}\,\varepsilon_{cs,j}\left(T_3 - T_{co,j+1}\right) \tag{8}$$

$$\varepsilon_{cs,j} = 1 - \exp\left(-NTU_{cs,j}\right);\ NTU_{cs,j} = \frac{U_{cs,j}\, A_{cs,j}}{\dot{m}_{co}\, c_{p,co}} \tag{9}$$

The condenser total power output, condenser heat and total heat transfer area are, respectively:

$$\dot{Q}_{cd} = \dot{Q}_{ds} + \sum_j \left(\dot{Q}_{cs,j}\right) + \dot{Q}_{sc};\ q_{cd} = \left(h_2 - h_5\right);\ A_{cd} = A_{ds} + \sum_j \left(A_{cs,j}\right) + A_{sc} \tag{10}$$

2.3.2 Pressure drop: The pressure drop at each control volume defines the pressure levels along the condenser. The pressure at the start of condensation, P_3, is adopted as the nominal condensing pressure.

$$P_{cd} = P_3;\ P_2 = P_3 + \Delta P_{ds};\ P_4 = P_3 - \sum_j \left(\Delta P_{cs,j}\right);\ P_5 = P_3 - \sum_j \left(\Delta P_{cs,j}\right) - \Delta P_{sc} \tag{11}$$

2.3.3 Degree of subcooling: The prescribed condenser outlet degree of subcooling provides:

$$\Delta T_{sc} = T_4 - T_5 \tag{12}$$

2.4 Expansion Device

An adiabatic thermostatic expansion valve, providing constant degree of superheat, was assumed. Therefore,

$$h_6 = h_5;\ T_1 = T_7 + \Delta T_{sh} \tag{13}$$

2.5 Evaporator

The evaporator is treated similarly to the condenser. Two control volumes, Fig. 4, are established, and the boiling zone is further divided into elements, to cope with local variation of the vapor quality.

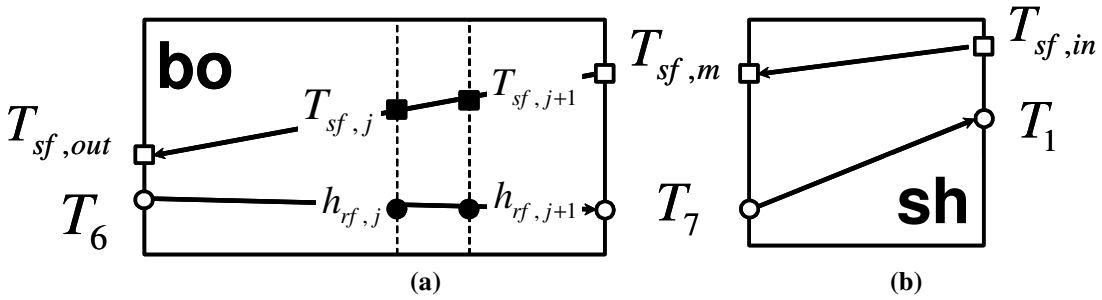

Figure 4: Control volumes for the evaporator (superheater, sh, and boiling, bo, zones), also showing the heat transfer element in the two-phase zone.

2.5.1 Heat transfer: The energy balances, heat transfer rate, effectiveness equations and overall heat transfer coefficient for the heat transfer element of the boiling zone are as follows:

$$\dot{Q}_{bo,j} = \dot{m}_{rf}\left(h_{rf,j+1} - h_{rf,j}\right);\ \dot{Q}_{bo,j} = \dot{m}_{sf}\, c_{p,sf}\left(T_{sf,j+1} - T_{sf,j}\right);\ \dot{Q}_{bo,j} = \dot{m}_{sf}\, c_{p,sf}\, \varepsilon_{bo,j}\left(T_{sf,j+1} - T_{rf,j}\right) \tag{14}$$

$$\varepsilon_{bo,j} = 1 - \exp\left(-NTU_{bo,j}\right);\ NTU_{bo,j} = \frac{U_{bo,j}\, A_{bo,j}}{\dot{m}_{sf}\, c_{p,sf}} \tag{15}$$

For the superheating zone, one has:

$$\dot{Q}_{sh} = \dot{m}_{rf}\left(h_1 - h_7\right);\ \dot{Q}_{sh} = \dot{m}_{sf}\, c_{p,sf}\left(T_{sf,in} - T_{sf,m}\right);\ \dot{Q}_{sh} = C_{\min,sh}\, \varepsilon_{sh}\left(T_{sf,i} - T_7\right) \tag{16}$$

Equations (9), for the determination of the effectivenesses of the condenser single-phase zones, also apply to the evaporator superheating zone. The total refrigeration capacity, refrigerant effect and evaporator total heat transfer area are, respectively:

$$\dot{Q}_{ev} = \sum_j \left(\dot{Q}_{bo,j} \right) + \dot{Q}_{sh};\ q_{ev} = \frac{\dot{Q}_{ev}}{\dot{m}_{rf}};\ A_{ev} = \sum_j \left(A_{bo,j} \right) + A_{sh} \tag{17}$$

2.5.2 Pressure drop: Likewise, the nominal evaporating pressure is taken as the pressure at the evaporator entrance, and the pressure drops are

$$P_{ev} = P_6;\ P_7 = P_6 - \sum_j \left(\Delta P_{bo,j} \right);\ P_1 = P_7 - \Delta P_{sh} \tag{18}$$

2.6 Heat Transfer Coefficients and Friction Factors

2.6.1. Overall heat transfer coefficients: It is assumed, for all control volumes, that (i) heat exchangers present no fouling; (ii) the thermal resistance due to conduction across the inner tube wall is negligible; (iii) the overall heat transfer coefficients are based on the inner heat transfer area of the inner tube of the heat exchanger and (iv) refrigerant flows in the annular passage of both heat exchangers. The overall heat transfer coefficients for the single-phase control volumes, (sh), (ds) and (sc), and for the two-phase flow control volumes, (cs,j) and (bo,j) are, respectively:

$$U_{sh/ds/sc} = \left(\frac{1}{\alpha_{sf/co}} + \frac{D_{io,ev/cd}}{D_{ii,ev/cd}} \frac{1}{\alpha_{sh/ds/sc}} \right);\ U_{bo/cs,j} = \left(\frac{1}{\alpha_{sf/co}} + \frac{D_{io,ev/cd}}{D_{ii,ev/cd}} \frac{1}{\alpha_{bo/cs,j}} \right) \tag{19}$$

2.6.2. Heat transfer and friction factor correlations: Table 1 summarizes the correlations used for all possible flow conditions in the heat exchangers. In both condenser and evaporator, chosen to be of the double-tube type, refrigerant was assumed to flow in the annular passages. This left the nanofluid, either as secondary fluid in the evaporator or condenser coolant, to flow in the circular conduit, a geometry for which nanofluid pressure drop and heat transfer studies are more readily available. For laminar single-phase internal flow of the base-fluid through a circular tube, the Fanning friction factor and the Nusselt number, $Nu = \alpha D/k$, were calculated assuming fully developed flow, with $\mathrm{Re} = \left(\dot{m}\ D \right) / \left(A_c\ \mu \right)$. For turbulent regime, equally assuming fully developed flow and uniform wall temperature, the friction factor and Nusselt number correlations from Bhatti and Shah (1987) and Pethukov and Popov (1963), respectively, were adopted. The Nusselt number in the transition regime is calculated from a linear interpolation between the Nusselt number values at the laminar and turbulent limits of the Reynolds number that are 2000 and 8000, respectively. For the Fanning friction factor, these limits vary slightly, to 2100 and 4000, respectively (Bhatti and Shah, 1987). As far as single-phase internal flow of a nanofluid through a circular tube is concerned, recent reviews from Kakaç and Pramuanjaroenkij (2009) and Godson et al. (2010) conclude that further theoretical and experimental work is needed to comprehensively understand the heat transfer mechanism. It is believed that the Dittus-Boelter (1930) correlation tends to underpredict the heat transfer (Yu et al., 2008). Godson et al. (2010) list convective heat transfer correlations for nanofluids from five investigations, three of which (Pak and Cho, 1998; Maïga et al., 2005; Maïga et al., 2006) make direct use of the traditional Dittus-Boelter (1930) correlation format, with different values for coefficient and exponents. In the present model, the correlation from Pak and Cho (1998), $Nu = 0.021\ \mathrm{Re}^{0.8}\ \mathrm{Pr}^{0.5}$, and the two-component nonhomogeneous equilibrium model from Buongiorno (2006) were equally tested. Pressure drop on the nanofluid side was calculated in the same way as for any other fluid (Xuan and Roetzel, 2000). For the refrigerant side, adequate correlations were chosen for single and two-phase flow in annular passages.

2.7 Refrigerant Properties

Equations (20) to (23) represent the refrigerant thermodynamic functions here employed, taken, in the present work, directly from the libraries of the EES (Engineering Equation Solver) platform.

$$h_1 = \underline{h}(T_1, P_1);\ \ v_1 = \underline{v}(T_1, P_1);\ \ s_1 = \underline{s}(T_1, P_1) \tag{20}$$

$$h_{2s} = \underline{h}(s_{2s}, P_2);\ T_2 = \underline{T}(h_2, P_2) \tag{21}$$

$$T_{cd} = \underline{T}_{sat}(P_{cd});\ \ h_3 = \underline{h}(x=1, P=P_3);\ T_4 = \underline{T}(x=0, P_4);\ \ h_4 = \underline{h}(x=0, P=P_4);\ T_5 = \underline{T}(h_5, P_5) \tag{22}$$

$$T_7 = \underline{T}(x=1, P=P_7);\ \ h_7 = \underline{h}(x=1, P=P_7) \tag{23}$$

Table 1: Choices of friction factor and heat transfer correlations for different control volumes

Control Volume	Fluid	Flow	Friction Factor Correlation	Heat Transfer Correlation	Conduit Geometry
CD	**Base-fluid**	laminar	$f\,\mathrm{Re} = 16$	$Nu = 4.364$	**Circular**
		turbulent	Bhatti and Shah (1987)	Pethukov and Popov (1963)	
	Nanofluid	laminar	$f\,\mathrm{Re} = 16$	$Nu = 4.364$	
		turbulent	Bhatti and Shah (1987)	Pak and Cho (1998) Xuan and Li (2003)	
EV	**Base fluid**	laminar	$f\,\mathrm{Re} = 16$	$Nu = 4.364$	
		turbulent	Bhatti and Shah (1987)	Pethukov and Popov (1963)	
	Nanofluid	laminar	$f\,\mathrm{Re} = 16$	$Nu = 4.364$	
		turbulent	Bhatti and Shah (1987)	Two-component nonhomogeneous equilibrium model, Buongiorno (2006)	
BO_j	**Refrigerant**	two-phase	Shah and Sekulic (2003)	Shah (1982)	**Annular**
CS_j		two-phase		Shah (1979)	
DS		laminar and turbulent	Bhatti and Shah (1987)	Laminar: $Nu = 4.364$ Turbulent: Gnielinski (1976)	
SC					
SH					

2.8 Nanofluid Characterization

2.8.1 Thermal conductivity: The thermal conductivity was calculated following the comprehensive work of Buongiorno et al. (2009), which reports measurements taken from identical samples of nanofluids by over 30 institutions worldwide. An important finding was that Maxwell´s model (1881), equation (24), for spherical and well-dispersed particles, generalized by Nan et al. (1997), to include particle geometry and finite interfacial thermal resistance, would provide thermal conductivity predictions in good agreement with experimental data.

$$\xi_k = \frac{k_{nf}}{k_{bf}} = \frac{k_{np} + 2k_{bf} + 2\phi_{np}\left(k_{np} - k_{bf}\right)}{k_{np} + 2k_{bf} - \phi_{np}\left(k_{np} - k_{bf}\right)} \tag{24}$$

2.8.2 Viscosity: In the absence, at the time of writing, of a generalized correlation for viscosity of nanofluids (Kole and Dey, 2010), specific correlations for each nanofluid had to be employed, such as the examples in equations (25), for H_20-Al_2O_3, from Pak and Cho (1998), and H_20-Cu, from Chen et al. (2007). Note that these correlations allow for an asymptotic value equal, or close, to that of the base fluid when ϕ_{np} tends to 0.

$$\xi_\mu = \frac{\mu_{nf(H_2O-Al_2O_3)}}{\mu_{bf(H_2O)}} = \left(1 + 39.11\phi_{np} + 533.9\phi_{np}^2\right);\ \xi_\mu = \frac{\mu_{nf(H_2O-Cu)}}{\mu_{bf(H_2O)}} = \left(0.995 + 36.45\phi_{np} + 468.72\phi_{np}^2\right) \tag{25}$$

2.8.3 Other properties: Density and specific heat are determined based on mass and energy balances, respectively, assuming for the latter that nanoparticle and base fluid are in thermal equilibrium (Khanafer and Vafai, 2011).

$$\rho_{nf} = \rho_{np}\phi_{np} + \rho_{bf}\left(1-\phi_{np}\right);\ c_{p,nf} = \frac{\phi_{np}\,\rho_{np}\,c_{p,np} + \left(1-\phi_{np}\right)\rho_{bf}\,c_{p,bf}}{\rho_{nf}} \tag{26}$$

3. NUMERICAL SOLUTION

The resulting non-linear system of algebraic equations was solved in the EES (Engineering Equation Solver) platform. The boiling (BO) and condensing (CS) control volumes required, as mentioned earlier, their division into small elements, of equal enthalpy increments, to cope with the variation of the local heat transfer coefficient. Since the two zones act as pure counter flow heat exchangers, sequential iterative procedures had to be established. Basically, the algorithm of these procedures starts with a guessed value of the heat transfer fluid outlet temperature. Convergence check and correction, $x_{i+1} = f\left(x_i\right)$, were carried out after each sequence. Moreover, since the boiling heat transfer coefficient depends on the Boiling number, which, by its turn, depends on the still unknown heat flux of the element, an additional inner loop had to be inserted. Convergence of the program depended mostly on the robustness of the heat pump input data. For this purpose, an additional EES program was developed to test or to produce coherent input values. Grid tests carried out with typical input data indicated a variation in the cooling capacity of a refrigeration system below 0.5% for an increase from 20 to 50 elements per two-phase zone.

Input data for the simulation included the rotational speed and geometry of the compressor (swept volume or, if reciprocating, bore and stroke), geometry of the heat exchangers (inner and outer diameters of both inner and outer cylinders, and length), refrigerant type, nanofluid characteristics (base fluid and nanoparticle material, size and volume fraction), mass flow rates and inlet states of condenser and evaporator heat transfer fluids, evaporator degree of superheating and condenser degree of subcooling. Simulation main results included: (i) compressor – refrigerant mass flow rate, power consumption and discharge temperature; (ii) condenser and evaporator – thermal capacities, heat transfer fluids and refrigerant outlet states, condensing and evaporating temperatures, refrigerant pressure drops and area distribution amongst heat exchanger zones; (iii) system – coefficient of performance and its enhancement factor, each one defined as follows:

$$COP_h = \left(\dot{Q}_{cd}/\dot{W}_{cp}\right);\ \xi_{COPh} = \left(COP_{h,nf}/COP_{h,bf}\right) \tag{27}$$

4. RESULTS

Figures 5a and 5b show preliminary results obtained with the simulation model for a liquid-to-liquid 19kW-nominal capacity heat pump. One observes that the heating coefficient of performance, depicted by the enhancement factor, increases with the volume fraction. Improved heat transfer conditions within the condenser resulted in a reduced condensing pressure thus improving the heating coefficient of performance. Note that the thermal conductivity enhancement of 6.1%, for a volume concentration of 2%, impacts the heat pump coefficient of performance in 5.4%. This difference is explained by the fact that viscosity also increases with nanoparticle volume fraction, while specific heat decreases, and that other thermal resistances in the condenser (predominantly refrigerant-side convection) come into play, all of them somehow affecting the overall heat transfer mechanism.

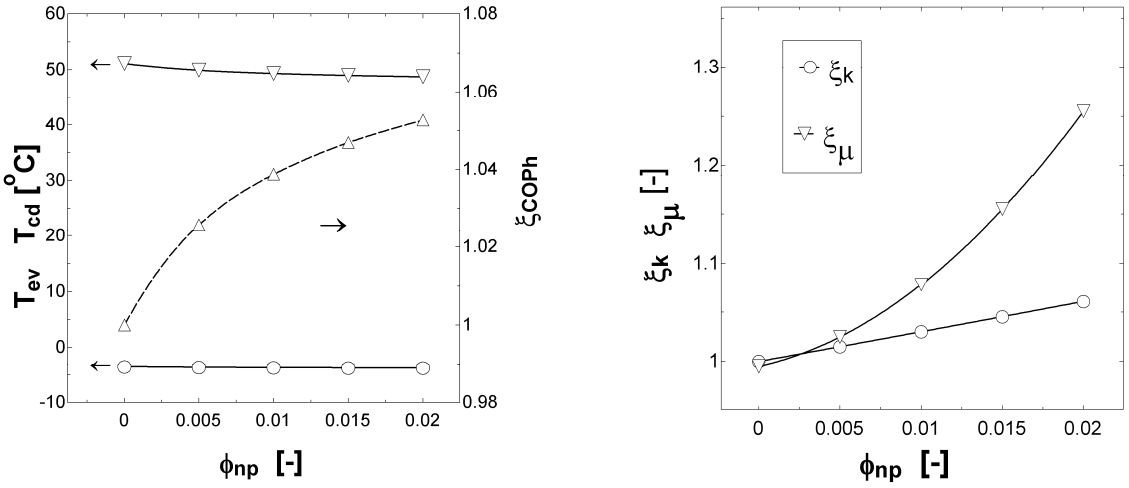

Figure 5: Variation with nanoparticle volume fraction of (a) condensing and evaporating temperatures and COP_h enhancement factor; (b) viscosity and thermal conductivity enhancement factors.

5. CONCLUSIONS

The following conclusions can be drawn from the present work:

- Thermal conductivity, viscosity and density of the nanofluid increase with volume fraction;
- The thermal conductivity enhancement of the condenser coolant may impact positively the heat pump coefficient of performance, although other thermal resistances in the condenser, as well as the viscosity enhancement, may attenuate such an increase;
- Although not shown in this work, the choice of the heat transfer correlation does affect the final results;
- Nanofluid increased pumping power (due to enhanced viscosity), degrading stability and fouling may become operational issues and have not been addressed, of course, in the present model;
- Experimental work should be carried out, to verify the findings of the present simulation.

NOMENCLATURE

A	area, m^2
A_c	cross sectional area, m^2
a_i	coefficients of volumetric efficiency eqn.
b_i	coefficients of isentropic efficiency equation
Bo	Boiling number, -
C_{max}	maximum capacity rate, kW K^{-1}
C_{min}	minimum capacity rate, kW K^{-1}
COP_h	heating coefficient of performance, -
C^*	capacity rate ratio, -
c_p	specific heat at constant pressure, kJ kg^{-1} K^{-1}
c_v	specific heat at constant volume, kJ kg^{-1} K^{-1}
D	diameter, m
D_h	hydraulic diameter, m
D_p	piston diameter (reciprocating), m
f	fanning friction factor, -
h	specific enthalpy, kJ kg^{-1}
$\underline{h}$	specific enthalpy function
h_{lv}	latent heat, kJ/kg
k	thermal conductivity, kW m^{-1} K^{-1}
$\dot{m}$	mass flow rate, kg s^{-1}
N `	compressor rotational speed, rpm
n_p	number of pistons (reciprocating)
NTU	number of transfer units, -
Nu	Nusselt number, -
P	pressure, kPa
Pr	Prandtl number, -
q''	heat flux, kW m^{-2}
$\dot{Q}$	heat transfer rate, kW
Re	Reynolds number

s	specific entropy, kJ kg^{-1} K^{-1}
$\underline{s}$	specific entropy function
s_p	compressor stroke (reciprocating), m
T	temperature, K
$\underline{T}$	temperature function
$\underline{T}_{sat}$	saturation (dew point) temperature function
U	overall heat transfer coefficient, kW m^{-2} K^{-1}
UA	conductance, kW K^{-1}
v	specific volume, m^3 kg^{-1}
$\underline{v}$	specific volume function
$\dot{V}_{cp}$	compressor displacement rate, m^3 s^{-1}
w_{cp}	compressor work, kJ kg^{-1}
$\dot{W}_{cp}$	compressor power, kW
x	vapour quality, -

Greek symbols

α	heat transfer coefficient, kW m^{-2} K^{-1}
$\bar{\alpha}$	zone averaged heat transf. coeff., kW m^{-2} K^{-1}
γ	specific heat ratio, -
ΔP	pressure drop, kPa
ΔT_{sc}	degree of subcooling, K
ΔT_{sh}	degree of superheating, K
ε	effectiveness, -
ϕ_{np}	volume fraction, -
η_{em}	electric motor efficiency, -
η_s	isentropic efficiency, -
η_v	volumetric efficiency, -
μ	dynamic viscosity, kg m^{-1} s^{-1}
ξ	enhancement factor, -
θ_p	pressure ratio, -
ρ	density, kg m^{-3}

Subscripts

a	cond. coolant state leaving sub-cooling zone
b	cond. coolant state leaving condensing zone
bf	base fluid
bo	boiling
cd	condenser
co	condenser coolant
cp	compressor
cs	condensing
ds	desuperheating
eq	equivalent
ev	evaporating
f	friction
i	relative to zone *i*
ii	inner tube inner surface
io	inner tube outer surface
in	inlet
j	relative to element *j*
l	liquid
m	secondary fluid state at boiling zone inlet
nf	nanofluid
np	nanoparticle
out	outlet
rf	refrigerant
s	isentropic
sc	subcooling
sf	secondary fluid
sh	superheating
v	vapour
1	compressor suction
2	compressor discharge
3	vapour (dew point) in CD
4	sat. liquid (bubble point) in CD
5	subcooled liquid outlet of CD
6	evaporator inlet
7	saturated vapour (dew point) in EV

REFERENCES

Bhatti, M. S., and R. K. Shah, 1987, Turbulent and transition convective heat transfer in ducts, in Handbook of Single-Phase Convective Heat Transfer, S. Kakaç, R. K. Shah, and W. Aung, eds., Wiley, New York, Chap. 4.

Brown, J. S., Yana-Motta, S. F., Domanski, P.A., 2002, Comparative analysis of automotive air conditioning systems operating with CO2 and R134a, *International Journal of Refrigeration*, vol. 25, pp. 19-32.

Buongiorno, J., 2006, Convective Transport in Nanofluids, *J. Heat Transfer ASME*, vol. 128, pp. 240-250.

Buongiorno, J., et al., 2009, A benchmark study on the thermal conductivity of nanofluids, *Journal of Applied Physics*, 106, 093412.

Chen, H., Ding, Y., He, Y., Tan, C., 2007, Rheological Behaviour of Ethylene Glycol Based Titania Nanofluids, *Chemical Physics Letters*, 444, 4, pp. 333-337.
Cheng L., Bandarra Filho, E. P., Thome, J. R., 2008, Nanofluid Two-Phase Flow and Thermal Physics: A New Research Frontier of Nanotechnology and its Challenges, *Journal of Nanoscience and Nanotechnology*, 8:1-18.
Choi, S. U. S., 1995, Developments and applications of non-newtonian flows, edited by D. D. Singer and H. P. Wang, American Society of Mechanical Engineering, New York, FED-Vol. 231/MD-vol. 66, p.99.
Dittus, P. W., Boelter, L. M. K., 1930, Heat Transfer in Automobile Radiators of the tubular type, *Univ. Calif. Pub. Eng.*, pp. 443-461.
Gnielinski, V., 1976, New equations for heat and mass transfer in turbulent pipe and channel flow, *International Chemical Engineering*, vol. 16, pp. 359-368.
Godson, L., Raja, B., Lal, D. M., Wongwises, S., 2010, Enhancement of heat transfer using nanofluids - An overview, *Renewable and Sustainable Energy Reviews*, vol. 14, pp. 629-641.
Kakaç, S., Pramuanjaroenkij, A., 2009, Review of convective heat transfer enhancement with nanofluids, *International Journal of Heat and Mass Transfer*, vol. 52, pp. 3187–3196.
Khanafer, K., Vafai, K., 2011, A critical synthesis of thermophysical characteristics of nanofluids, *Int. J. Heat Mass Transfer*, vol. 54, pp. 4410-4428.
Kole, M., Dey, T.K., 2010, Viscosity of alumina nanoparticles dispersed in car engine coolant, *Experimental Thermal and Fluid Science*, 34, 677–683.
Loaiza, J. C. V., Pruzaesky, F. C., Parise, J A. R., 2010, A Numerical Study on the Application of Nanofluids in Refrigeration Systems, International Refrigeration and Air Conditioning Conference. Paper 1145.
Maïga, S. E. B., Nguyen C.T., Galanis N., Roy G., Maré T., Coqueux M., 2006, Heat transfer enhancement in turbulent tube flow using Al2O3 nanoparticle suspension, *International Journal of Numerical Methods for Heat and Fluid Flow*, 16(3):275–292.
Maïga, S. E. B., Palm S. J., Nguyen C. T., Roy G., Galanis N., 2005, Heat transfer enhancements by using nanofluids in forced convection flows, *International Journal of Heat and Fluid Flow*, vol. 26, pp. 530–546.
Martins Costa, M. L., Parise, J. A. R., 1993, A three-zone simulation model for a air-cooled condensers, *Heat Recovery Systems and CHP*, Volume 13, Issue 2, pp. 97-113.
Maxwell, J.C., 1881, A Treatise on Electricity and Magnetism, 2nd edition, Claredon, Oxford.
Nan, C.W., Birringer, R., Clarke, D.R., Gleiter, H., 1997, Effective thermal conductivity of particulate composites with interfacial thermal resistance, *Journal of Applied Physics*, 81, 6692-6699.
Pak, B. C., Cho, Y. I., 1998, Hydrodynamic and Heat Transfer Study of Dispersed Fluids with Submicron Metallic Oxide Particles, *Experimental Heat Transfer*, Vol. 11, No. 2, pp. 151-170.
Parise, J. A. R., 2010, A Seven-control Volume Simulation Model for the Vapor Compression Refrigeration Cycle, *Proc. MERCOFRIO, Congresso de Climatização e Refrigeração*, paper MF10-0039, Porto Alegre, Brazil.
Petukhov, B. S., and V. N. Popov, 1963, Theoretical calculation of heat exchange in turbulent flow in tubes of an incompressible fluid with variable physical properties, *High Temp.*, Vol. 1, No. 1, pp. 69–83.
Sarkar, J., 2011, A critical review on convective heat transfer correlations of nanofluids, *Renewable Sustainable Energy Rev.*, vol. 15, pp. 3271-3277.
Shah, M. M., 1979, A general correlation for heat transfer during film condensation inside pipes, *International Journal of Heat and Mass Transfer,* vol., 22, pp. 547-556.
Shah, M. M., 1982, Chart correlation for saturated boiling heat transfer: equations and further study, *ASHRAE Trans.*, vol. 88, pp. 185-196.
Shah, R.K., Sekulic, D. S., 2003, Fundamentals of Heat Exchanger Design, John Wiley and Sons, USA, 972 pages.
Xuan, Y., Li, Q., 2003, Investigation on Convective Heat Transfer and Flow Features of Nanofluids, *Journal of Heat Transfer,* vol. 125, pp. 151-155.
Xuan, Y., Roetzel, W., 2000, Conceptions for heat transfer correlation of nanofluids*, International Journal of Heat and Mass Transfer*, vol. 43, pp. 3701-3707.

ACKNOWLEDGEMENTS

Thanks are due to CAPES, CNPq and FAPERJ, Brazilian research funding agencies, for the financial support. The author is indebted to Dr. Yipsy R. Benito, for her contribution to the literature review in nanofluids, and also to Prof. Jacopo Buongiorno (MIT, Cambridge, MA) and Prof. Andrew D. Sommers (Miami University, Oxford, OH) who kindly provided the authors with valuable information at key points of the project.